Biomaterials Science

ROYAL SOCIETY OF CHEMISTRY

PAPER

View Article Online
View Journal | View Issue

Cite this: *Biomater. Sci.*, 2022, **10**, 4902

Analysis of the potential role of photocurable hydrogel in patient-derived glioblastoma organoid culture through RNA sequencing†

Lun Liang, ‡ Run Cui,‡ Sheng Zhong, Zhenning Wang, Zhenqiang He, Hao Duan, Xiaoyu Guo, Jie Lu, Hongrong Hu, Chang Li, Chengwei Yu, Yanjiao Yu, Chengcheng Guo* and Yonggao Mou*

Patient-derived glioblastoma organoid (GBO) growth in hydrogels recapitulates key features of parental tumors, making GBOs a useful tool for fundamental research on cancer biology and offer deeper insight into the development of innovative therapeutic strategies for cancer treatment. Matrigel as a natural hydrogel has been widely used for 3D culture in most tumor organoid studies, but the volatility in its biochemical and biophysical properties makes it difficult to be further applied in GBO cultures. Thus, several kinds of biomimetic hydrogels from synthetic or biological polymers have been developed for tumor organoid growth. Here, we innovatively utilize a photocurable hydrogel-based biomimetic instructive system containing gelatin methacryloyl (GelMA) mixed with a hyaluronic acid (HA) hydrogel as a scaffold for generating GBOs. Furthermore, we evaluated the GBO biological properties at the transcriptome level, which showed that GBOs cultured with this hydrogel retain the expression profile of key neurodevelopmental markers, driving mutations and alternative splicing of parental tumors. Notably, GBOs cultured with the photocurable hydrogel may provide a platform for precision cancer medicine, bridging the gap between basic research and clinical application. Although significant challenges remain, biomimetic hydrogels can provide an exceptional window for the construction of tumor organoids to ensure the accuracy of the research and clinical data.

Received 15th April 2022,
Accepted 23rd June 2022

DOI: 10.1039/d2bm00589a

rsc.li/biomaterials-science

Introduction

Glioblastoma (GBM) is the most common primary malignant brain tumor in adults and is associated with poor outcomes.[1] The median survival of newly diagnosed glioblastoma after the use of conventional therapies is approximately 16 to 20 months.[2] Currently, no effective anti-tumor drugs are available for GBM treatment due to the heterogeneous and invasive nature of glioblastoma and the limitations of traditional drug screening methods. The classical method for drug screening is culturing cancer cells in a 2D plate. However, cancer cells present poor intratumor heterogeneity during 2D culturing and gradually lose the characteristics of the parental tumor.[3,4] Cancer organoids have been widely used in recent times for screening and efficacy evaluation of drugs to explore personalized treatment strategies.[5] Jacob *et al.* reported that patient-derived glioblastoma organoids (GBOs) can maintain the key features of parental tumors, including their histological features, cellular diversity, gene expression, and mutational profiles. These findings provide a basis for the development of patient-specific treatment strategies and drug screening.[6]

GBOs can be cultured with and without hydrogels.[6,7] Matrigel has been widely used in GBO culture.[8] A previous study reported that GBOs cultured with Matrigel (containing exogenous EGF/bFGF) demonstrated stem cell heterogeneity and a hypoxic gradient.[7] However, Matrigel contains more than 1800 unique proteins,[9] making it difficult to control the specific needs for organoid structure and function during the culture. In the culture system, mechanical properties have great effects on organoid development.[10] The mechanical properties of Matrigel have been found to be heterogeneous and the elastic moduli of local regions are several times higher than the average modulus of the sample.[11,12] Methacrylated gelatin (GelMA), synthesized by grafting methacrylate groups onto the amine-containing side groups of gelatin, has been

Department of Neurosurgery/Neuro-oncology, Sun Yat-sen University Cancer Center, State Key Laboratory of Oncology in South China, Collaborative Innovation Center for Cancer Medicine, Guangzhou 510000, China. E-mail: guochch@sysucc.org.cn, mouyg@sysucc.org.cn

†Electronic supplementary information (ESI) available. See DOI: https://doi.org/10.1039/d2bm00589a

‡These authors contributed equally to this work.

widely used in tissue engineering and several biomedical applications.[13] Furthermore, GelMA-based hydrogels have been increasingly studied for nerve tissue engineering.[14] Recent studies have shown that the nerve guidance conduits of GelMA-based hydrogel can promote nerve regeneration.[15,16] Besides, GelMA has been proved to have good temperature stability and a low swelling ratio to maintain its mechanical properties.[17] A study showed that 5% (w/v) GelMA has high ductility and favorable compression resistance, biomimetic shear modulus, and toughness, making it a potential material for disc degeneration repair.[18] Erkoc *et al.* cultured a glioblastoma cell line U373 with GelMA hydrogels, and the results indicated that U373 presented a significantly high expression of the pro-survival gene Bcl-2 and low expression levels of the pro-apoptotic genes, Bad, Puma and caspase-3. These findings indicate that GelMA may act as an extracellular matrix (ECM) to promote the growth of glioblastoma.[19] In summary, the advantages of GelMA hydrogels include favorable biological properties, easily modified physical characteristics, and the presence of cell binding and matrix metalloproteinase-responsive peptide motifs.[20] Hyaluronic acid (HA) is the most abundant component of ECM in the healthy brain tissue.[21] HA regulates tissue mechanics and hydration as well as activates cellular signalling through surface receptors such as CD44.[22,23] Previous studies show that the tumour and stromal cells secrete HA in high-grade gliomas.[24,25] Furthermore, low molecular weight HA promotes tumour invasion, while high molecular weight HA reduces tumour invasion.[26,27] Tang M. *et al.* generated a 3D glioblastoma model using a mixture of 4% GelMA and 0.25% glycidyl methacrylate–HA (GMHA) as the ECM composition exhibiting cellular dependencies and immune interactions in vitro.[28] However, some methods for generating GBOs involve directly cutting tumor tissues into pieces without hydrogels.[6,29] Notably, cutting tumor tissue removes ECM and potentially alters the tumor microenvironment and may limit the application of these methods. Therefore, hydrogels were used as ECM to culture GBOs in the present study. Few studies have explored the use of GelMA and HA in GBOs culture. In addition, the biological characteristics of GBOs have not been fully elucidated.

In the current study, a GBOs culture method was developed by combining pieces of tumor tissues with a mixture of 5% (w/v) GelMA and 0.25% (w/v) HA as the ECM. We selected the recipes of the hydrogel, based on several previous studies, which demonstrated that 5% (w/v) GelMA-supported cell survival and proliferation, of which viability was more than 90%.[30–32] Besides, when compared with 10% and 15% (w/v) GelMA, the pore size of 5% (w/v) GelMA was maximum, which might allow the cells to be in good contact with the medium.[33] 0.25% (w/v) HA was used to mimic the ECM composition of glioblastoma, which has been reported by Tang, M *et al.*[28] The second group of GBOs was cultured without hydrogels to act as the control group. Tumor tissue sample processing and GBOs culture were performed as described in a previous study.[29] RNA-sequencing analysis was performed to explore expression profiles of the key genes after GBOs culture. Furthermore, a system was developed by RNA sequencing analysis to evaluate the biological characteristics of GBOs, including analysis of differentially expressed genes (DEGs), single-nucleotide polymorphism (SNP), alternative splicing (AS), expression levels of drug target genes, infiltration of immune cells, tumor microenvironment (TME) score and genetic expression tendency. The findings of the present study provide a basis for the development of personalized therapy for GBM patients.

Materials and methods

Tumor samples

Collection, dissection, and processing of tumor samples were performed as described in a previous study.[29] Fresh tumor samples were obtained from a 60-year-old female patient diagnosed with recurrent glioblastoma through surgical resection. Tissue samples were washed with sterile phosphate-buffered saline at 4 °C and cut into small slices of 1–2 mm diameter in a glioblastoma dissection medium.[29] Tumor slices were prepared for GBOs culture. Written informed consent was obtained from the participant, prior to the surgery.

GBO culture

GBO medium was prepared as described previously.[29] A mixture of 10% (w/v) GelMA (EFL-GM-60, Suzhou, China) and 0.5% (w/v) HA (EFL-HA-150K, Suzhou, China) was heated in a water bath at 70 C for 20 min under dark conditions. The hydrogels were then immediately filtered with a 0.45 μm sterile needle filter. The hydrogels were heated at 37 °C after filtration. The hydrogels were mixed with equal volumes GBO medium containing pieces of tumor and extruded through a syringe (to obtain 5% (w/v) GelMA and 0.25% (w/v) HA). The mixture was subjected to 405 nm blue light irradiation curing for 30 seconds to complete the GBO production (Fig. 1). Pieces of tumors were cultured without hydrogels as a control group. Two groups of GBOs were cultured with a GBO medium in a 5.0% CO_2 incubator at 37 °C.

RNA-sequencing analysis

Hydrogels were cleaved with GelMA lysate (EFL-GM-LS-001 Suzhou, China) to release the tumor tissue before RNA extraction. Total RNA was extracted using a TRIzol reagent kit (Invitrogen, Carlsbad, CA, USA). RNA quality was assessed using an Agilent 2100 Bioanalyzer (Agilent Technologies, Palo Alto, CA, USA) and RNase-free agarose gel electrophoresis was performed. Eukaryotic mRNA was enriched using Oligo(dT) beads, whereas prokaryotic mRNA was enriched by removing rRNA using Ribo-ZeroTM Magnetic Kit (Epicentre, Madison, WI, USA). The enriched mRNA was fragmented into short fragments using a fragmentation buffer and reverse transcribed into cDNA with random primers. Second-strand cDNA was synthesized using DNA polymerase I, RNase H, dNTP, and a buffer. The cDNA fragments were then purified with a QiaQuick PCR extraction kit (Qiagen, Venlo, The Netherlands), end-repaired, poly(A) added, and ligated to Illumina sequencing adapters. The ligation products were size selected by

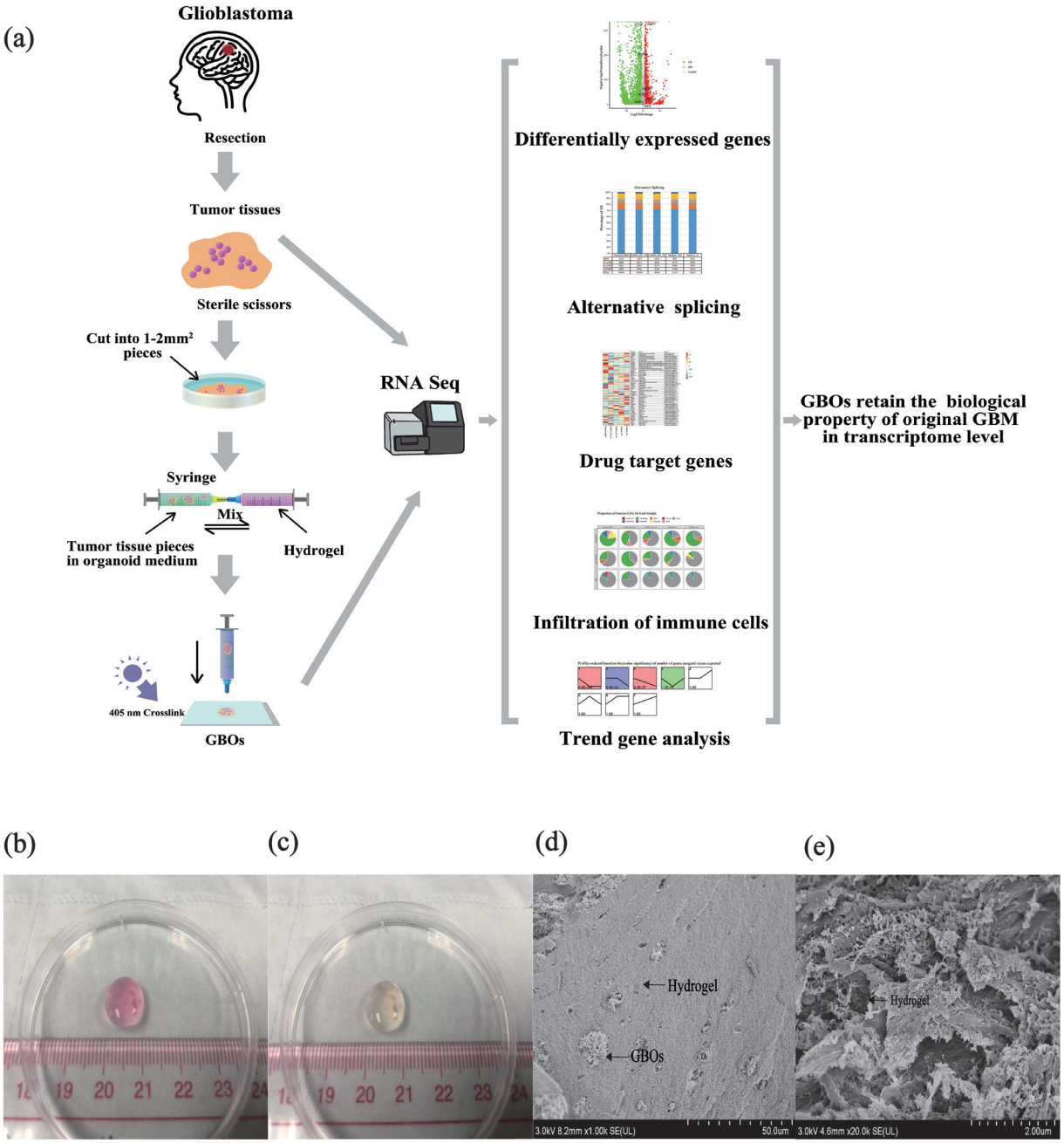

Fig. 1 A schematic representation of the process of making GBOs with hydrogels. (a) Fresh tumor samples were cut into pieces and mixed with hydrogels. (b) GBOs combined with hydrogels before 405 nm blue light crosslink. (c) GBOs with hydrogels after 405 nm blue light crosslink. (d and e) Scanning electron microscopy (SEM) analysis of GBOs with hydrogels.

agarose gel electrophoresis, PCR amplified, and sequenced using Illumina HiSeq2500 at the Gene Denovo Biotechnology Co. (Guangzhou, China).

Differentially expressed genes (DEGs)

RNAs differential expression analysis between the two samples was performed using the edgeR package in R Studio.[34] Genes/transcripts with a false discovery rate (FDR) below 0.05 and absolute fold change ≥1 were considered differentially expressed genes. FDR also called *Q* value, is the corrected *P*-value, which is a stricter test threshold compared with *P*-value.

Single-nucleotide polymorphism (SNP) analysis

The GATK tool[35] (version 3.4–46) was used for calling variants of transcripts, and ANNOVAR was used for SNP/InDel annotation. Function, genome site, and type of variation of SNPs were also analyzed.

Alternative splicing analysis

The rMATS[36] (version 4.0.1) software (https://rnaseq-mats.sourceforge.net/index.html) was used to identify alternative splicing events and analyze differential alternative splicing events between samples. AS events with a false discovery rate (FDR) < 0.05 were selected as significant AS events. The classification of alternative splicing was performed as follows: SE: skipped exon; MXE: mutually exclusive exon; A5SS: alternative 5′ splice site; A3SS: alternative 3′ splice site; RI: retained intron.

Immune cell infiltration and tumor microenvironment analysis

Immune cell infiltration analysis was performed using TIMER2.0,[37] a free web server for data analysis (https://timer.cistrome.org/). Tumor microenvironment analysis was performed using the ESTIMATE tool.[38]

Drug target and relevance genes analysis

Drug targets of glioblastoma were retrieved from TTD (Therapeutic Target Database, https://db.idrblab.net/ttd/)[39] and OncoKB (https://www.oncokb.org/levels) database.[40]

Trend analysis, KEGG pathway enrichment analysis and GO (gene ontology) enrichment analysis

Trend analysis is a method to cluster the gene expression patterns of multiple continuous samples (at least 3 samples). The clustering results can show the trend of gene set expression, such as increasing, decreasing, or no change in expression. Trend analysis was performed by the short time-series Expression Miner[41] software. The files of the gene expression (in the order of 0, 7, and 14 days) were input into the software. KEGG Pathway and GO enrichment analyses were performed using OmicShare tools, a free online platform for data analysis (https://www.omicshare.com/tools). Expression data for each sample were normalized to 0, log2 (v1/v0), log2 (v2/v0), and then clustered using Short Time-series Expression Miner software (STEM).[42] GO/KEGG enrichment analysis was performed for genes in each trend, and the *p*-value was calculated through hypothesis testing. The *p*-value obtained was corrected by FDR[43] and a Q value ≤ 0.05 was used as the threshold for determining significantly enriched GO terms and pathways.

Scanning electron microscopy (SEM) analysis

GBOs with hydrogels were incubated in 2.5% glutaraldehyde solution overnight at 4 °C. The samples were then washed thrice with 0.1 M, pH7.0 phosphate buffer, each time taking 15 minutes. Samples were fixed with 1% osmic acid solution for 2 hours and then washed with 0.1 M, pH 7.0 phosphate buffer. Samples were dehydrated with gradient concentrations of ethanol (including 30%, 50%, 70%, 80%, 90%, 95% and 100%) for 20 minutes at each concentration. Further, samples were treated with a mixture of epoxy embedding agent and acetone (1 : 1) (v/v) for 1 h, a mixture of epoxy embedding agent and acetone (3 : 1) (v/v) for 3 h, and pure epoxy embedding agent overnight. The samples were sliced using a LEICA EM UC7 ultra-thin slicer to obtain 70–90 nm slices. The slices were stained with lead citrate and dioxy acetate for 5 min and then dried for photogenic observations.

Results

Glioblastoma organoids (GBOs) culture

The traditional tumor organoid culture is mainly characterized by the division of tumor tissue into single cells, which is not conducive to preserving native cell-to-cell interactions. A method for directly separating tumor tissue into small pieces was recently developed for culturing GBOs. However, we considered that this method might result in the loss of ECM after cutting tumor samples. Thus, tumor tissue sections were mixed with hydrogels (5% GelMA and 0.25% HA) to generate GBOs to circumvent this limitation (Fig. 1).

Effect of GBOs on the expression of neurodevelopmental marker genes

Analysis of differentially expressed genes (DEGs) was performed using a panel of neurodevelopmental marker genes, including glioma stem cell marker genes SOX2 and OLIG2, glial marker genes GFAP and S100B, neural progenitor marker genes NES, HOPX andFABP7 and the cell proliferation marker gene MKI67 to characterize cellular identities between the parental tumor (original GBM) and GBOs (Fig. 2). The immunofluorescence staining details are shown in Fig. S1.† Although some of these markers were maintained by GBOs, the expression levels changed significantly during the culture (Fig. 2a). When the gene expression level of GBOs was no different or higher than that of the parental tumor, it indicated that GBOs maintained the gene expression profile. When the gene expression level of the organoid was lower than that of the parental tumor, it implied that the GBOs did not maintain the gene expression. This definition was also applied to subsequent drug target analysis. GBOs combined with hydrogels maintained the expression levels of FABP7, SOX2, and KMI67 on day 7, whereas GBOs without hydrogels only maintained KMI67 expression on day 7 (Fig. 2a and c, Table S1†). The GBOs with hydrogels maintained HOPX expression on day 14, whereas, the GBOs without hydrogels did not maintain HOPX expression at this time point (Fig. 2e and f, Table S2†). Notably, no genes showed lower expression levels in GBOs with6 the hydrogel group than in the GBOs without the hydrogel group (Fig. 2d and g, Tables S1 and S2†). These results indicate that the hydrogels played a significant role in maintaining some neurodevelopmental marker genes in GBOs. However, the expression of GFAP and S100B was not maintained in the two groups (Fig. 2b, c, e and f, Tables S1 and S2†).

Effects of GBOs on variants and alternative splicing

Although the number of variants type, location of variants, and alternative splicing in GBOs decreased compared with that of the parental tumor (Fig. 3a–d), the percentages in GBOs were similar to those in the parental tumor (Fig. 3b–d), except for the location of variants (Fig. 3a). The findings

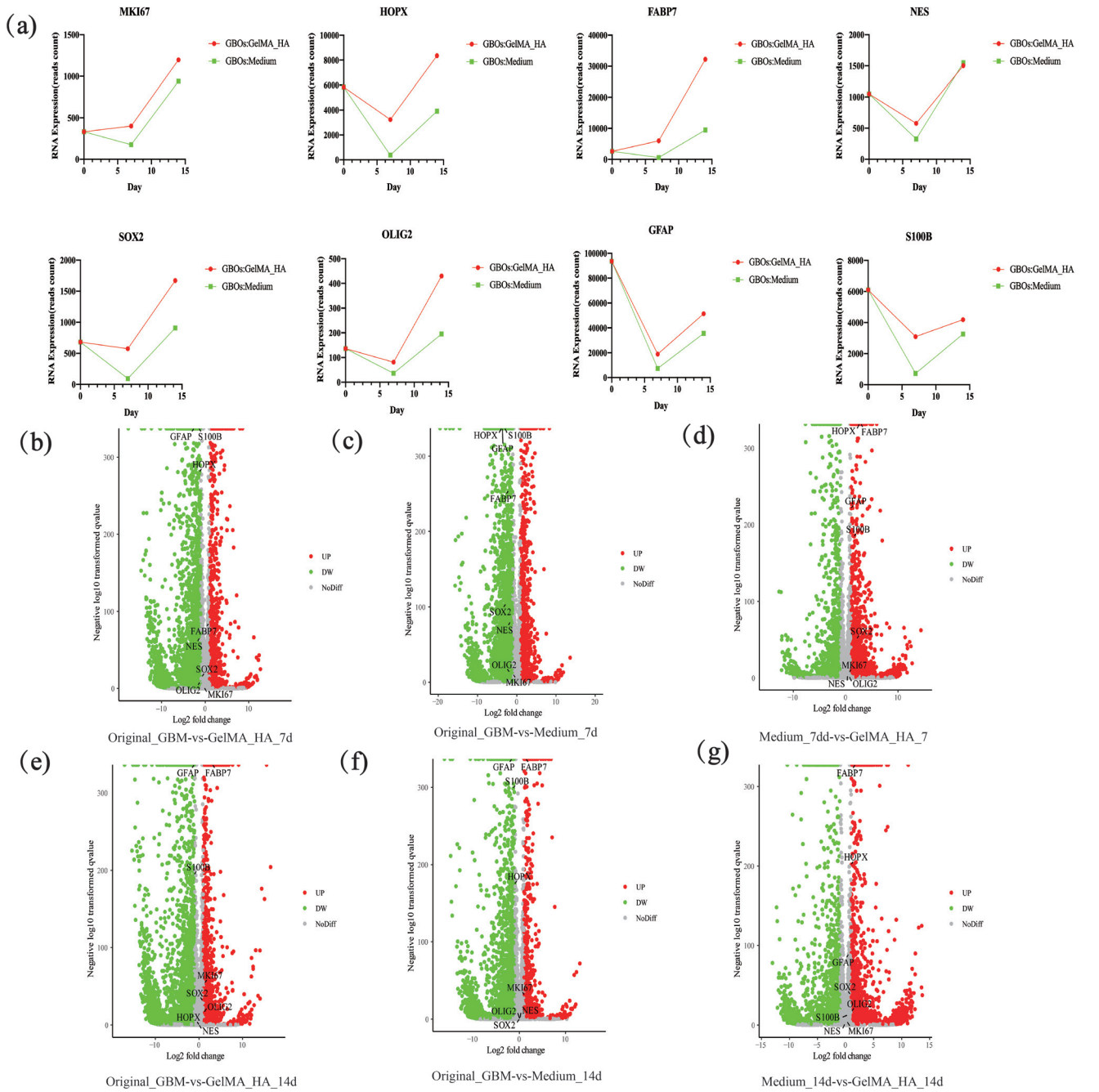

Fig. 2 Expression levels of neurodevelopmental marker genes in GBOs. (a) Changes in reads count of MKI67, HOPX, FABP7, NES, SOX2, OLIG2, GFAP and S100B during GBOs culture. (b–g) Volcano plots showing differentially expressed genes (DEGs) between two groups. False discovery rate (FDR) below 0.05 and absolute fold change ≥1 indicated differentially expressed genes. Original GBM was used as the control group for (b)/(c)/(e)/(f), medium_7d was used as the control group for (d) and medium_14d was used as the control group for (g).

showed no significant differentially expressed alternative splicing for approximately 70%–90% variants in GBOs compared with parental tumors, indicating that GBOs maintained most alternative splicing expression (Fig. 3e–h).

Effect of GBOs on drug target genes

The findings showed that the two types of GBOs maintained expression of the target genes PTEN, TNKS, MTOR, CDK12, and NF1 on day 7 (Fig. 4b and c, Table S1†). GBOs without hydrogels maintained FROM1 expression on day 7 whereas GBOs with hydrogels did not maintain the expression of FROM1 on day 7 (Fig. 4b and c, Table S1†). TNKS/CRBN was maintained by the two types of GBOs on day 14 (Fig. 4e and f, Table S2†). GBOs without hydrogels maintained PTEN/MTOR/CDK12 expression on day 14 whereas GBOs with hydrogels did not maintain expression of these genes (Fig. 4e and f,

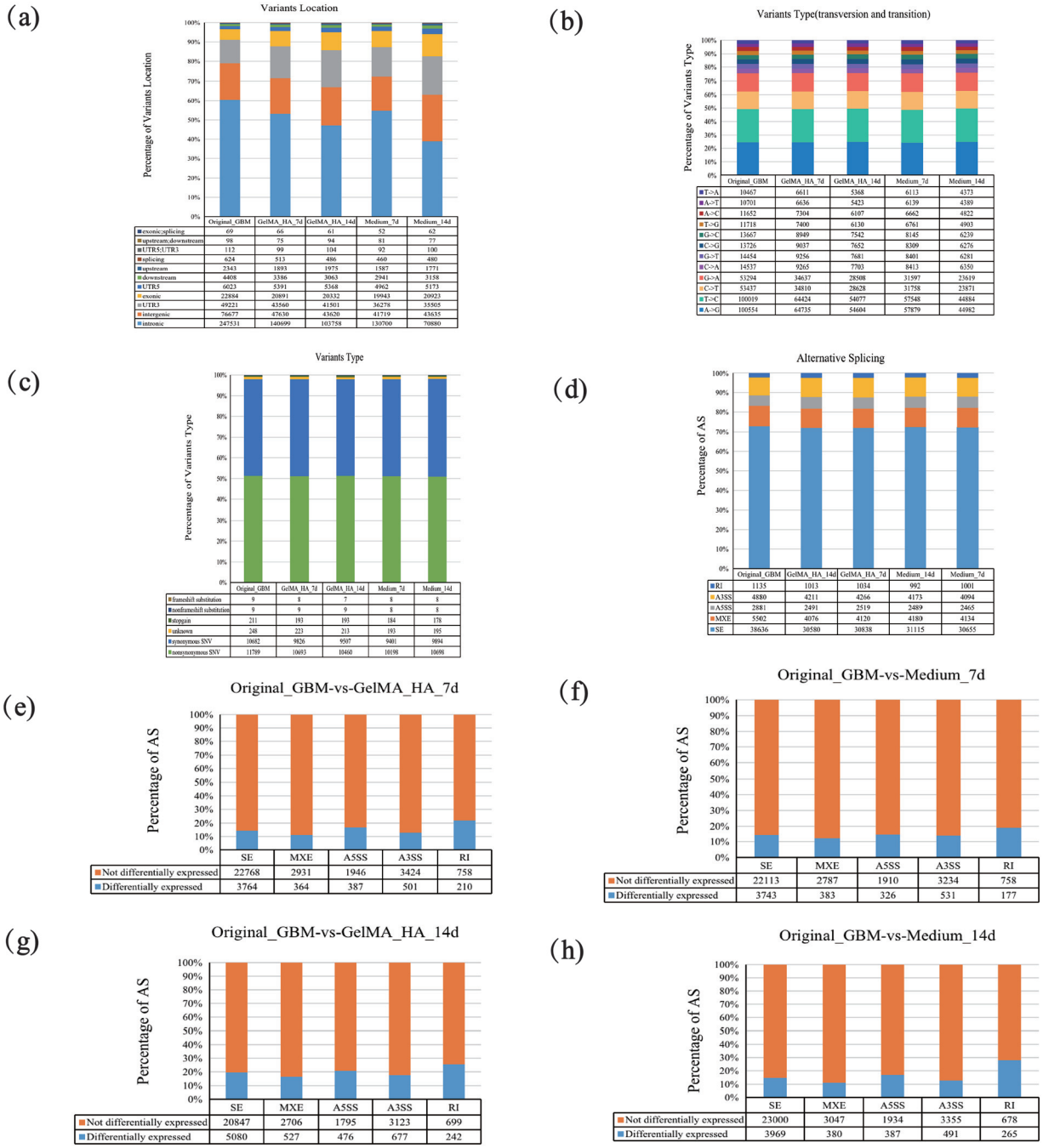

(a)	Original_GBM	GelMA_HA_7d	GelMA_HA_14d	Medium_7d	Medium_14d
exonic;splicing	69	66	61	52	62
upstream;downstream	98	75	94	81	77
UTR5;UTR3	112	99	104	92	100
splicing	624	513	486	460	480
upstream	2343	1893	1975	1587	1771
downstream	4408	3386	3063	2941	3158
UTR5	6023	5391	5368	4962	5173
exonic	22884	20891	20332	19943	20923
UTR3	49221	43560	41501	36278	35505
intergenic	76677	47630	43620	41719	43635
intronic	247531	140699	103758	130700	70880

(b)	Original_GBM	GelMA_HA_7d	GelMA_HA_14d	Medium_7d	Medium_14d
T->A	10467	6611	5368	6113	4373
A->T	10701	6636	5423	6139	4389
A->C	11652	7304	6107	6662	4822
T->G	11718	7400	6130	6761	4903
G->C	13667	8949	7542	8145	6239
C->G	13726	9037	7652	8309	6276
G->T	14454	9256	7681	8401	6281
C->A	14537	9265	7703	8413	6350
G->A	53204	34637	28508	31597	23619
C->T	53437	34810	28628	31758	23871
T->C	100019	64424	54077	57548	44884
A->G	100554	64735	54604	57879	44982

(c)	Original_GBM	GelMA_HA_7d	GelMA_HA_14d	Medium_7d	Medium_14d
frameshift substitution	9	8	7	8	8
nonframeshift substitution	9	9	9	8	8
stopgain	211	193	193	184	178
unknown	248	223	213	193	195
synonymous SNV	10682	9826	9507	9401	9894
nonsynonymous SNV	11789	10693	10460	10198	10698

(d)	Original_GBM	GelMA_HA_14d	GelMA_HA_7d	Medium_14d	Medium_7d
RI	1135	1013	1034	992	1001
A3SS	4880	4211	4266	4173	4094
A5SS	2881	2491	2519	2489	2465
MXE	5502	4076	4120	4180	4134
SE	38636	30580	30838	31115	30655

(e)	SE	MXE	A5SS	A3SS	RI
Not differentially expressed	22768	2931	1946	3424	758
Differentially expressed	3764	364	387	501	210

(f)	SE	MXE	A5SS	A3SS	RI
Not differentially expressed	22113	2787	1910	3234	758
Differentially expressed	3743	383	326	531	177

(g)	SE	MXE	A5SS	A3SS	RI
Not differentially expressed	20847	2706	1795	3123	699
Differentially expressed	5080	527	476	677	242

(h)	SE	MXE	A5SS	A3SS	RI
Not differentially expressed	23000	3047	1934	3355	678
Differentially expressed	3969	380	387	491	265

Fig. 3 Maintenance of variants and alternative splicing by GBOs. (a–d) Composition and proportion of variants type, location and alternative splicing in parental tumor and GBOs. (e–h) Differentially expressed alternative splicing between parental tumor and GBOs. Original GBM was used as the control group and a false discovery rate (FDR) < 0.05 indicated significant as events.

Table S2†). GBOs with hydrogels retained EGFR expression on day 14, whereas GBOs without hydrogels did not maintain the EGFR expression at this time point (Fig. 4e and f, Table S2†). EGFR was a classic drug target gene for treating glioblastoma, and the expression of EGFR in GBOs with hydrogels was higher than GBOs without hydrogels on both day 7 and day 14 (Fig. 4d and g, Tables S1 and Table S2†). These results indicated that GBOs with hydrogels and GBOs without hydrogels had some differences in maintaining the expression of drug target genes.

Effect of GBOs on immune cells

Analysis of immune cell infiltration showed that macrophages had the highest proportion in GBOs and parental tumors. However, the proportion of other immune cells was different between the parental tumors and GBOs (Fig. 5a). Infiltration

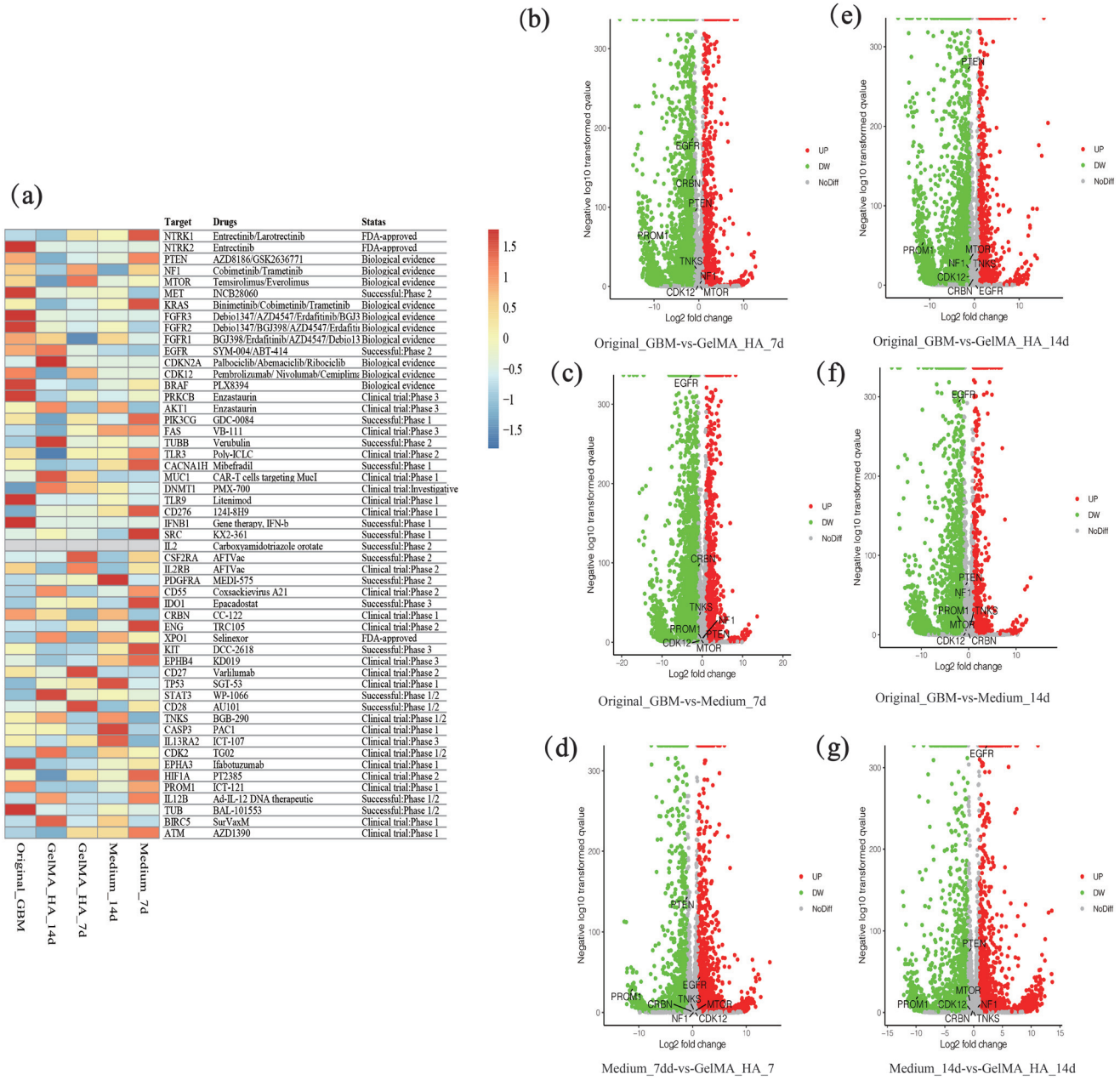

Fig. 4 Effect of GBOs on expression levels of drug target genes. (a) Heat map showing the expression level of drug target genes in parental tumor and GBOs. (b–g) Volcano plots showing differentially expressed genes (DEGs) between samples. False discovery rate (FDR) below 0.05 and absolute fold change ≥1 indicated differentially expressed genes. Original GBM was used as the control group for (b)/(c)/(e)/(f), medium_7d was used as the control group for (d). Medium_14d was used as the control group for (g).

scores of immune cells given by various algorithms were different, making it difficult to assess the level of infiltration (Fig. 5b). Tumor microenvironment scores, including immune score, stroma score, and estimate score were used to assess the overall degree of infiltration of immune cells, stroma cells, and purity of the tumor cells. The immune score of GBOs with hydrogels was higher than that of GBOs without hydrogels on days 7 and day 14, whereas the estimated score of GBOs with hydrogels was lower on day 14 (Fig. 5c and e). These results indicated that GBOs with hydrogels resulted in higher infiltration of immune cells relative to GBOs without hydrogels.

Gene expression profile during GBOs culture

Analyses in the previous part of this study were mainly based on inter-sample factors. Trend analysis was performed to explore the dynamic changes in gene expression between the two types of GBOs. The parental tumor (original GBM) was set as day 0 of GBOs culture and the gene expression pattern was clustered according to the gene expression level on day 0, day

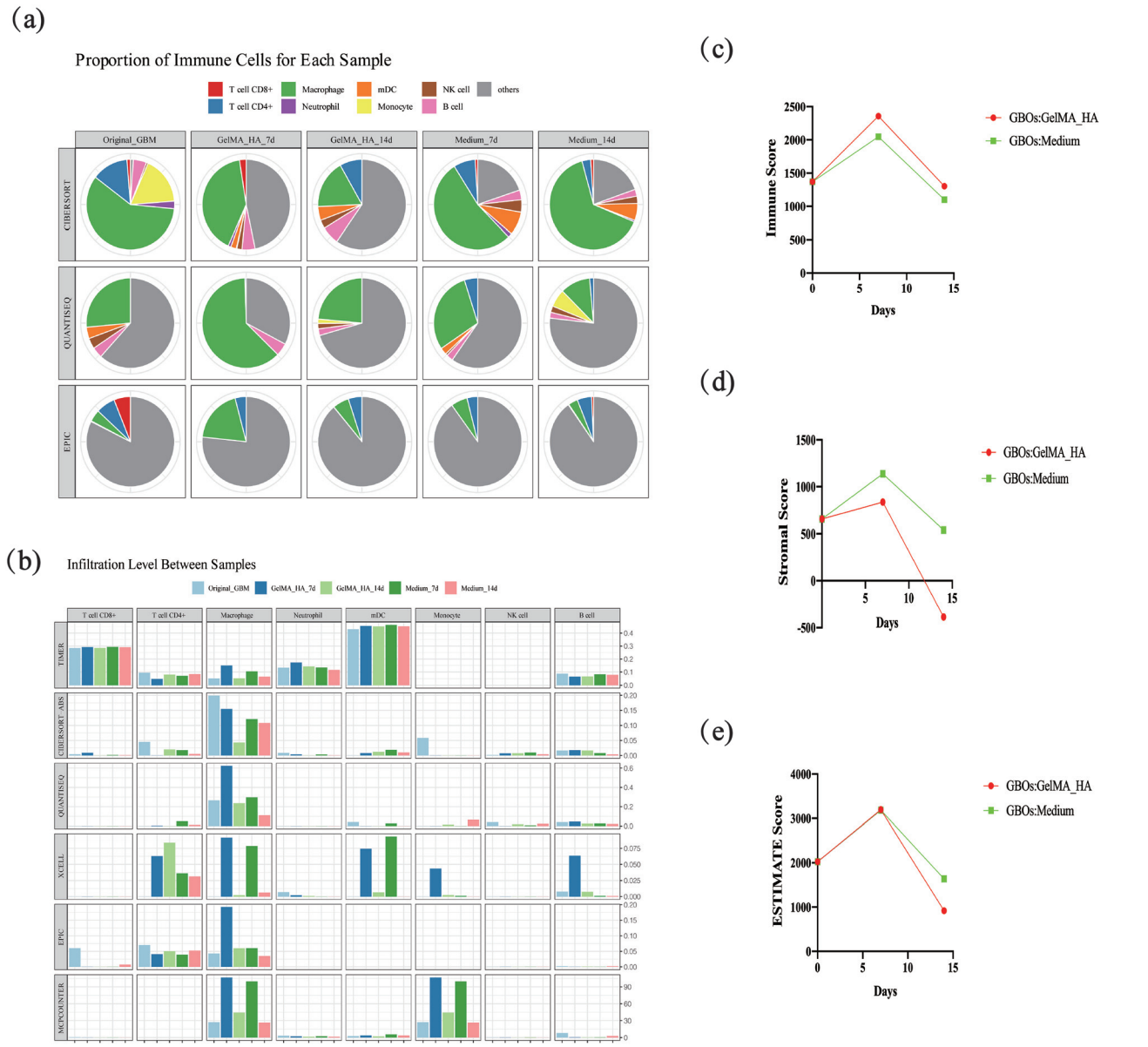

Fig. 5 Effect of GBOs on infiltration of immune cells. (a and b) Proportion and infiltration of immune cells in parental tumor and GBOs as determined using the TIMER2.0 tool. (c–e) Stromal score, immune score and estimate score on day 0 (parental tumor), day 7 and day 14 during GBO culture.

7, and day 14. Genes were defined as "Trend Genes" and "No Trend Genes" in the trend analysis. "No Trend Genes" represented stably expressed genes, whereas "Trend Genes" represented genes with unstable expression during culture. The number of "Trend Genes" in GBOs with the hydrogel group was approximately 2.23 times the number of "No Trend Genes" (Fig. 6a). The number of "Trend Genes" in GBOs without the hydrogel group was about 1.57 times the number of "No Trend Genes" (Fig. 6b) This finding indicated that a higher number of genes changed their expression during the process of GBOs culture compared with the number of genes that had a stable expression (Fig. 6a and b). The biological process classification comprised the top 20 GO terms of "No Trend Genes" in all GBOs, whereas the cellular component comprised the top 20 GO terms of "Trend Genes" in all GBOs (Fig. 6c–f). The top 20 GO terms of "No Trend Genes" (Fig. 6c and e) and "Trend Genes" (Fig. 6d and f) between GBOs with hydrogels and GBOs without hydrogels were different. KEGG pathway enrichment analysis showed that the main pathways of "No Trend Genes " in GBOs with hydrogels were "osteoclast differentiation" and "lysosome" (Fig. 7a), whereas, the most enriched pathway in GBOs without hydrogels was "Cytokine–cytokine receptor interaction" (Fig. 7c). "Calcium signal pathway" was the most enriched pathway of "Trend Genes" in all GBOs (Fig. 7b and d). Venn diagram was generated to further explore the similarities and differences in GO terms and KEGG pathways between GBOs with hydrogels and GBOs without hydrogels (Fig. 7e and f, Tables S3 and S4†). The IL-17

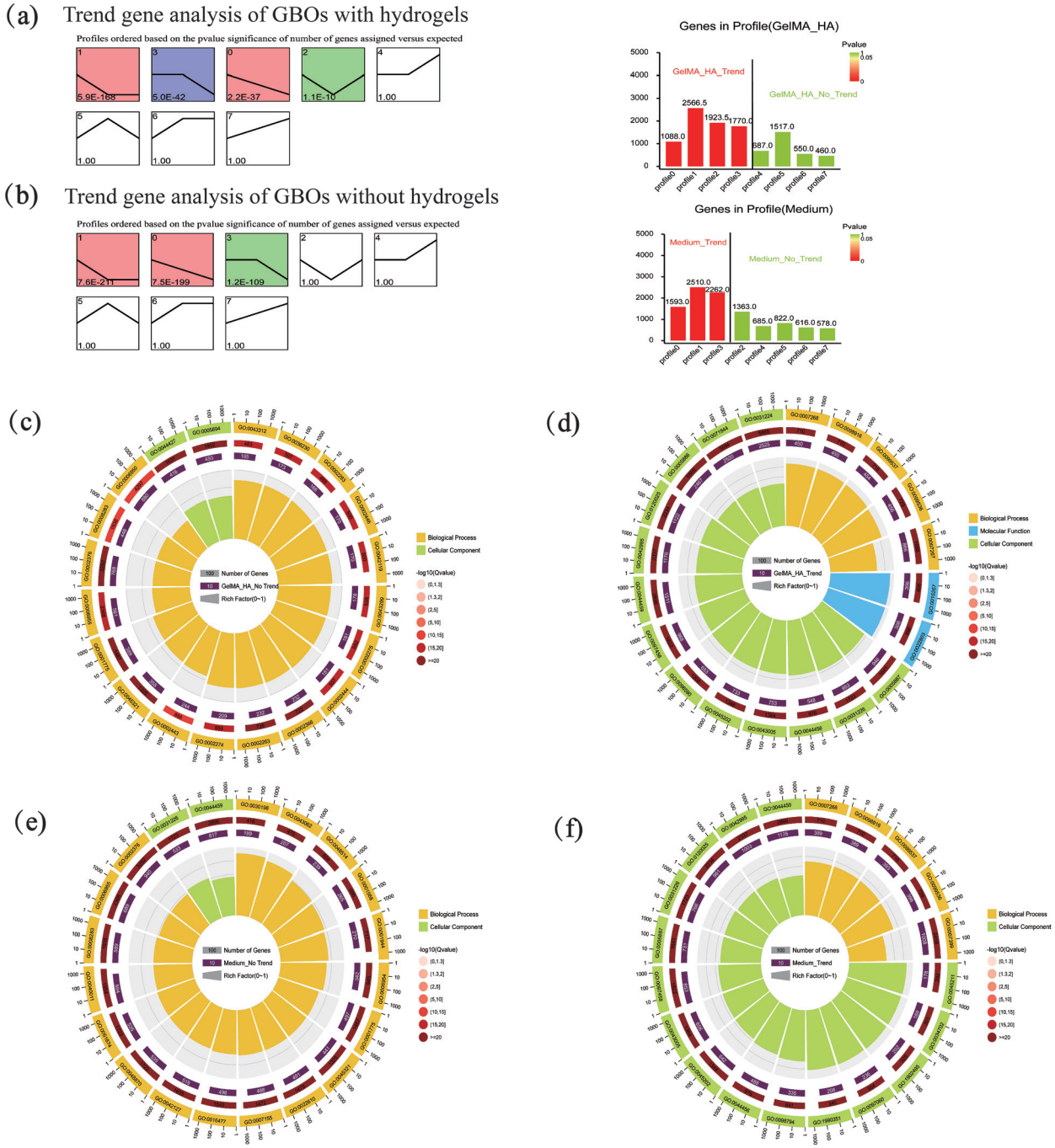

Fig. 6 Trend analysis of GBOs during culture. (a and b) Trend analysis of GBO with hydrogels (GelMA–HA) and GBOs without hydrogels (medium). The profiles are shown on the left. Red, blue and green profiles represent trend genes and white profiles represent no trend genes. The number of trend genes and no trend genes are shown on the right. (c) Top 20 GO enrichment terms of no trend genes in GBOs with hydrogels. (d) Top 20 GO enrichment terms of trend genes in GBOs with hydrogels. (e) Top 20 GO enrichment terms of no trend genes in GBOs without hydrogels. (f) Top 20 GO enrichment terms of trend genes in GBOs without hydrogels.

signaling pathway, apoptosis, and cell cycle pathways were stably expressed in GBOs with hydrogels, whereas, pathways in cancer and focal adhesion were significantly enriched in GBOs without hydrogels. TNF signaling pathway and chemokine signaling pathways were significantly enriched in the two types of GBOs (Fig. 7e, Table S3†). The chromosomal part, the mitotic cell cycle process and DNA metabolic process terms were significantly enriched in GBOs with hydrogels, whereas B cell differentiation and response to endogenous stimuli were significantly enriched in GBOs without hydrogels. The immune system process, cell activation, and inflammatory response were significantly enriched in GBOs with and without hydrogels (Fig. 7f, Table S4†).

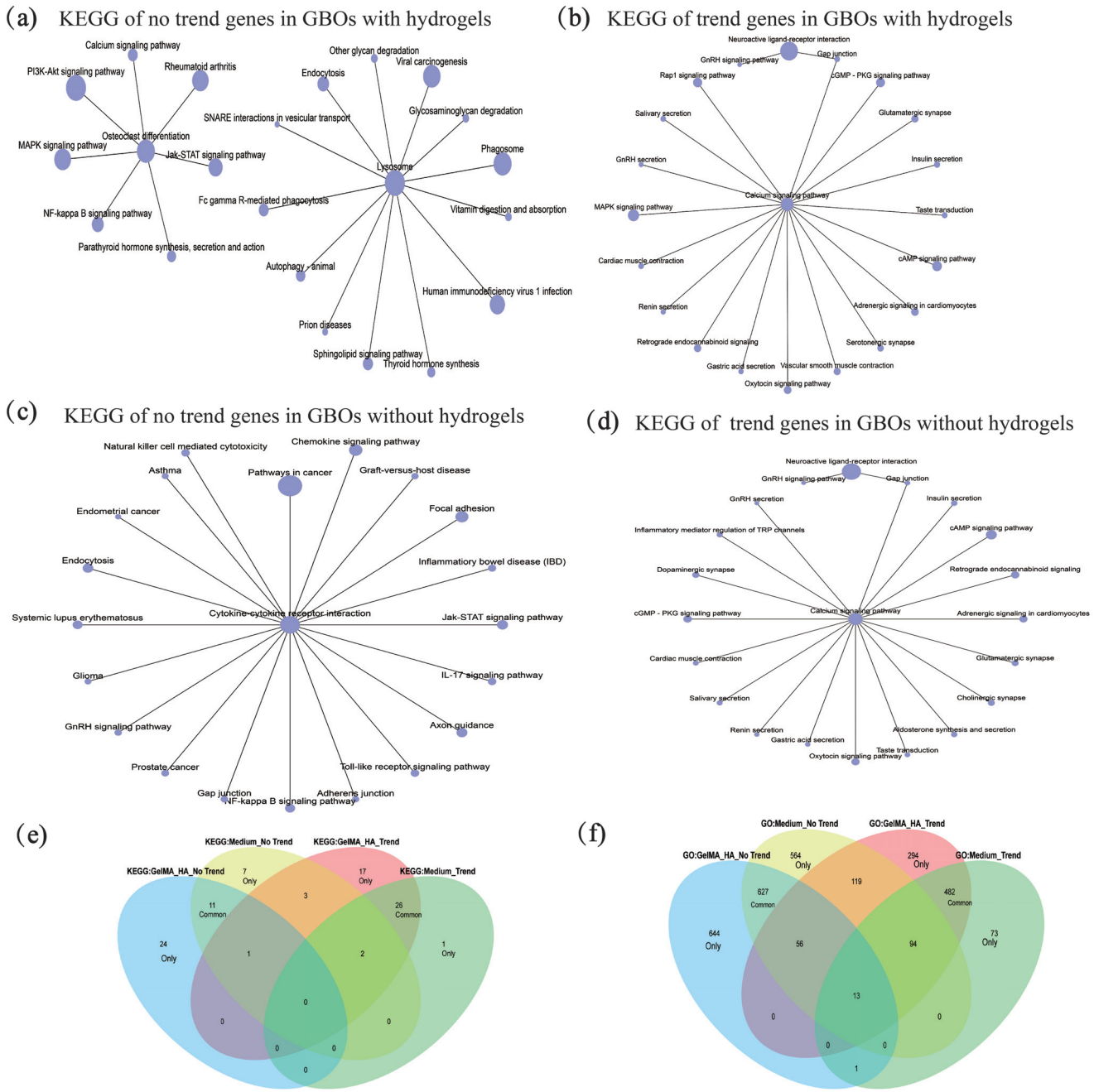

Fig. 7 KEGG pathway enrichment trend analysis and venn diagram of KEGG pathway/GO terms for trend analysis in GBOs. (a) Top 20 enriched KEGG pathways of no trend genes in GBOs with hydrogels. (b) Top 20 enriched KEGG pathways of trend genes in GBOs with hydrogels. (c) Top 20 enriched KEGG pathways of no trend genes in GBOs without hydrogels. (d) Top 20 enriched KEGG pathways of trend genes in GBOs without hydrogels. (e) Venn diagram of KEGG pathways of trend genes and no trend genes in GBOs. (f) Venn diagram of GO terms based on trend genes and no trend genes in GBOs.

Discussion

Recent studies reported that GBOs can be generated by cutting tumor tissue into pieces rather than using hydrogels and separating tumor tissue into cells. GBOs maintain the heterogeneity of parental tumors and the interactions between cells.[6,29] However, we consider this method may be associated with the loss of extracellular matrix. GelMA–HA hydrogels are mixed with tumor tissue pieces to overcome this limitation. In the present study, GBOs combined with hydrogels retained the characteristics of the parental tumor, such as glioma stemness and proliferation. Moreover, expression levels of MKI67 and SOX2 in GBOs with hydrogels were higher relative to the expression levels in GBOs without hydrogels. This implies that the use of hydrogel with 5% GelMA and 0.25% HA improves GBOs culture. Similar to our results, a previous study reported

that low molecular weight HA promotes GBM cell invasion and glioblastoma stem cell stemness.[44] This indicated that HA should be added to the ECM when generating GBOs. Furthermore, our GBOs were easy to make and it only took 30 seconds of UV light to crosslink the hydrogel. A system was established to evaluate the biological characteristics of GBOs through RNA-seq analysis. The advantages of the method are as follows: (1) analysis of differentially expressed genes showed that the expression of key genes was maintained by GBOs, (2) the percentages of single-nucleotide polymorphisms (SNPs), and alternative splicing (AS) of GBOs were similar to those of the parental tumor and most of them were maintained in the GBO group. Notably, these polymorphisms play an important role in regulating gene expression,[45,46] (3) drug target gene analysis indicated potential strategies for the development of personalized therapies, (4) analysis of immune cells infiltration showed key association with drug response providing a basis for the development of personalized therapies (such as immunotherapy) based on GBOs, (5) trend analysis showed dynamic changes in gene expression during the GBOs culture. "No trend genes" represent genes with stable expression during GBOs culture, thus the functions of these genes should be explored *in vitro*. Further analysis of these genes helps in the identification of potential targets for personalized therapies. GBOs without hydrogels were set as the control group to further explore whether the application of hydrogels promotes GBOs culture. GBOs with hydrogels and GBOs without hydrogels showed some similarities and differences. The two groups retained the expression of key genes in the parental tumor. Osteoclast differentiation and lysosome pathways were significantly enriched in the group comprising GBOs with hydrogels, whereas the cytokine–cytokine receptor interaction pathway was significantly enriched in GBOs without hydrogels. The present study had some limitations. HA was physically mixed with GelMA, which might lead to high biodegradation. Chemical and physical crosslinking were reported to surmount the high biodegradation.[47,48] In future studies, we will explore the ways to improve the stability of HA in GelMA, optimizing GelMA–HA mixed hydrogel. Besides, this was the first time a mixture of GelMA and HA was used to generate GBOs, therefore, tumor samples were collected from one patient. In addition, GBOs were cultured only for two weeks. Further studies should explore the application of GBOs using samples from more patients and evaluate the effect of long-term culture of GBOs. Although the macrophage level was maintained by the GBOs used in the current study, the level of macrophages decreased over time. This is because the culture conditions were optimized to preserve tumor cell viability rather than the viability of immune cells, which was consistent with findings reported in a previous study.[6]

Conclusions

GelMA–HA hydrogels were mixed with patient-derived tumor tissue pieces to establish a method for making GBOs. The GBOs with the hydrogels maintained the parental tumor features, such as the expression of key genes. Furthermore, a system for evaluating GBOs through RNA-seq analysis was developed to explore the biological characteristics of GBOs, which deepens our understanding of GBOs.

Ethical approval

The study was approved by the Ethics Committee of Sun Yat-sen University Cancer Center. Permit No. GZR-2018244 and was performed in accordance with the ethical standards as laid down in the 1964 Declaration of Helsinki and its later amendments or comparable ethical standards in 2008 (5). Informed consent was obtained from all patients for being included in the study.

Author contributions

L. L. and R. C. contributed equally to this work. L. L. and R. C. designed the overall experimental plan and wrote the manuscript. S. Z., Z. W., Z. H., D. H., X. G., and J. L. performed the experiments. H. H., C. L., C. Y., and Y. Y. were involved in the data analysis. C. G. and Y. M. supervised the project, conceived the original idea, and revised the manuscript.

Conflicts of interest

The authors declare no conflicts of interest.

Acknowledgements

This work was supported by grants from the National Natural Science Foundation of China (NSFC), project number: 81872324; Guangzhou Science and Technology and Information Bureau, grant number: 201704020133; Jiangmen Science and Technology Bureau, grant number: 2018630100110019805; Youth Fund of National Natural Science Foundation of China, grant number: 81802498. Guangdong Frontier and Key Technology Innovation Project (grant number: 2015B010125003). We thank Dr Tao Xu and Dr Haiyan Chen for providing technical support in hydrogel synthesis. We also thank Home for Researchers editorial team (**https://www.home-forresearchers.com**) for the language editing service.

References

1 Q. T. Ostrom, H. Gittleman, G. Truitt, A. Boscia, C. Kruchko and J. S. Barnholtz-Sloan, *Neuro-Oncology*, 2018, **20**, iv1–iv86.
2 M. R. Gilbert, J. J. Dignam, T. S. Armstrong, J. S. Wefel, D. T. Blumenthal, M. A. Vogelbaum, H. Colman,

A. Chakravarti, S. Pugh, M. Won, R. Jeraj, P. D. Brown, K. A. Jaeckle, D. Schiff, V. W. Stieber, D. G. Brachman, M. Werner-Wasik, I. W. Tremont-Lukats, E. P. Sulman, K. D. Aldape, W. J. Curran Jr. and M. P. Mehta, *N. Engl. J. Med.*, 2014, **370**, 699–708.

3 S. E. Burdall, A. M. Hanby, M. R. Lansdown and V. Speirs, *Breast Cancer Res.*, 2003, **5**, 89–95.

4 J. Lee, S. Kotliarova, Y. Kotliarov, A. G. Li, Q. Su, N. M. Donin, S. Pastorino, B. W. Purow, N. Christopher, W. Zhang, J. K. Park and H. A. Fine, *Cancer Cell*, 2006, **9**, 391–403.

5 J. Kondo and M. Inoue, *Cells*, 2019, **8**(5), 470.

6 F. Jacob, R. D. Salinas, D. Y. Zhang, P. T. T. Nguyen, J. G. Schnoll, S. Z. H. Wong, R. Thokala, S. Sheikh, D. Saxena, S. Prokop, D. A. Liu, X. Qian, D. Petrov, T. Lucas, H. I. Chen, J. F. Dorsey, K. M. Christian, Z. A. Binder, M. Nasrallah, S. Brem, D. M. O'Rourke, G. L. Ming and H. Song, *Cell*, 2020, **180**, 188–204.

7 C. G. Hubert, M. Rivera, L. C. Spangler, Q. Wu, S. C. Mack, B. C. Prager, M. Couce, R. E. McLendon, A. E. Sloan and J. N. Rich, *Cancer Res.*, 2016, **76**, 2465–2477.

8 C. Zhang, M. Jin, J. Zhao, J. Chen and W. Jin, *Am. J. Cancer Res.*, 2020, **10**, 2242–2257.

9 C. S. Hughes, L. M. Postovit and G. A. Lajoie, *Proteomics*, 2010, **10**, 1886–1890.

10 S. Dahl-Jensen and A. Grapin-Botton, *Development*, 2017, **144**, 946–951.

11 J. Reed, W. J. Walczak, O. N. Petzold and J. K. Gimzewski, *Langmuir*, 2009, **25**, 36–39.

12 S. S. Soofi, J. A. Last, S. J. Liliensiek, P. F. Nealey and C. J. Murphy, *J. Struct. Biol.*, 2009, **167**, 216–219.

13 W. Schuurman, P. A. Levett, M. W. Pot, P. R. van Weeren, W. J. A. Dhert, D. W. Hutmacher, F. P. W. Melchels, T. J. Klein and J. Malda, *Macromol. Biosci.*, 2013, **13**, 551–561.

14 A. G. Kurian, R. K. Singh, K. D. Patel, J. H. Lee and H. W. Kim, *Bioact. Mater.*, 2022, **8**, 267–295.

15 X. Fang, H. Guo, W. Zhang, H. Fang, Q. Li, S. Bai and P. Zhang, *J. Mater. Chem. B*, 2020, **8**, 10593–10601.

16 W. Ye, H. Li, K. Yu, C. Xie, P. Wang, Y. Zheng, P. Zhang, J. Xiu, Y. Yang, F. Zhang, Y. He and Q. Gao, *Mater. Des.*, 2020, **192**, 108757.

17 L. Han, J. L. Xu, X. Lu, D. L. Gan, Z. X. Wang, K. F. Wang, H. P. Zhang, H. P. Yuan and J. Weng, *J. Mater. Chem. B*, 2017, **5**, 731–741.

18 H. Xu, M. Sun, C. Wang, K. Xia, S. Xiao, Y. Wang, L. Ying, C. Yu, Q. Yang, Y. He, A. Liu and L. Chen, *Biofabrication*, 2020, **13**(1), 015010.

19 P. Erkoc, F. Seker, T. Bagci-Onder and S. Kizilel, *Macromol. Biosci.*, 2018, **18**, 3.

20 K. Yue, G. Trujillo-de Santiago, M. M. Alvarez, A. Tamayol, N. Annabi and A. Khademhosseini, *Biomaterials*, 2015, **73**, 254–271.

21 D. R. Zimmermann and M. T. Dours-Zimmermann, *Histochem. Cell Biol.*, 2008, **130**, 635–653.

22 M. K. Cowman, H. G. Lee, K. L. Schwertfeger, J. B. McCarthy and E. A. Turley, *Front. Immunol.*, 2015, **6**, 261.

23 K. T. Dicker, L. A. Gurski, S. Pradhan-Bhatt, R. L. Witt, M. C. Farach-Carson and X. Q. Jia, *Acta Biomater.*, 2014, **10**, 1558–1570.

24 B. Delpech, C. Maingonnat, N. Girard, C. Chauzy, R. Maunoury, A. Olivier, J. Tayot and P. Creissard, *Eur. J. Cancer*, 1993, **29a**, 1012–1017.

25 K. C. Yoo, Y. Suh, Y. An, H. J. Lee, Y. J. Jeong, N. Uddin, Y. H. Cui, T. H. Roh, J. K. Shim, J. H. Chang, J. B. Park, M. J. Kim, I. G. Kim, S. G. Kang and S. J. Lee, *Oncogene*, 2018, **37**, 3317–3328.

26 T. Chanmee, P. Ontong and N. Itano, *Cancer Lett.*, 2016, **375**, 20–30.

27 X. Tian, J. Azpurua, C. Hine, A. Vaidya, M. Myakishev-Rempel, J. Ablaeva, Z. Y. Mao, E. Nevo, V. Gorbunova and A. Seluanov, *Nature*, 2013, **499**, 346–U122.

28 M. Tang, Q. Xie, R. C. Gimple, Z. Zhong, T. Tam, J. Tian, R. L. Kidwell, Q. Wu, B. C. Prager, Z. Qiu, A. Yu, Z. Zhu, P. Mesci, H. Jing, J. Schimelman, P. Wang, D. Lee, M. H. Lorenzini, D. Dixit, L. Zhao, S. Bhargava, T. E. Miller, X. Wan, J. Tang, B. Sun, B. F. Cravatt, A. R. Muotri, S. Chen and J. N. Rich, *Cell Res.*, 2020, **30**, 833–853.

29 F. Jacob, G. L. Ming and H. Song, *Nat. Protoc.*, 2020, **15**, 4000–4033.

30 B. Byambaa, N. Annabi, K. Yue, G. Trujillo-de Santiago, M. M. Alvarez, W. Jia, M. Kazemzadeh-Narbat, S. R. Shin, A. Tamayol and A. Khademhosseini, *Adv. Healthcare Mater.*, 2017, **6**, 16.

31 K. Chen, E. Jiang, X. Wei, Y. Xia, Z. Wu, Z. Gong, Z. Shang and S. Guo, *Lab Chip*, 2021, **21**, 1604–1612.

32 J. Yin, M. Yan, Y. Wang, J. Fu and H. Suo, *ACS Appl. Mater. Interfaces*, 2018, **10**, 6849–6857.

33 E. George, I. Jahan, A. Barai, V. Ganesan and S. Sen, *Biomed. Mater.*, 2021, **16**, 5.

34 M. D. Robinson, D. J. McCarthy and G. K. Smyth, *Bioinformatics*, 2010, **26**, 139–140.

35 P. Shannon, A. Markiel, O. Ozier, N. S. Baliga, J. T. Wang, D. Ramage, N. Amin, B. Schwikowski and T. Ideker, *Genome Res.*, 2003, **13**, 2498–2504.

36 M. I. Love, W. Huber and S. Anders, *Genome Biol.*, 2014, **15**, 550.

37 T. W. Li, J. X. Fu, Z. X. Zeng, D. Cohen, J. Li, Q. M. Chen, B. Li and X. S. Liu, *Nucleic Acids Res.*, 2020, **48**, W509–W514.

38 K. Yoshihara, M. Shahmoradgoli, E. Martinez, R. Vegesna, H. Kim, W. Torres-Garcia, V. Trevino, H. Shen, P. W. Laird, D. A. Levine, S. L. Carter, G. Getz, K. Stemke-Hale, G. B. Mills and R. G. W. Verhaak, *Nat. Commun.*, 2013, **4**, 2612.

39 Y. Zhou, Y. T. Zhang, X. C. Lian, F. C. Li, C. X. Wang, F. Zhu, Y. Q. Qiu and Y. Z. Chen, *Nucleic Acids Res.*, 2022, **50**, D1398–D1407.

40 D. Chakravarty, J. J. Gao, S. Phillips, R. Kundra, H. X. Zhang, J. J. Wang, J. E. Rudolph, R. Yaeger,

T. Soumerai, M. H. Nissan, M. T. Chang, S. Chandarlapaty, T. A. Traina, P. K. Paik, A. L. Ho, F. M. Hantash, A. Grupe, S. S. Baxi, M. K. Callahan, A. Snyder, P. Chi, D. C. Danila, M. Gounder, J. J. Harding, M. D. Hellmann, G. Iyer, Y. Y. Janjigian, T. Kaley, D. A. Levine, M. Lowery, A. Omuro, M. A. Postow, D. Rathkopf, A. N. Shoushtari, N. Shukla, M. H. Voss, E. Paraiso, A. Zehir, M. F. Berger, B. S. Taylor, L. B. Saltz, G. J. Riely, M. Ladanyi, D. M. Hyman, J. Baselga, P. Sabbatini, D. B. Solit and N. Schultz, *JCO Precis. Oncol.*, 2017, **2017**, PO.17.00011.

41 J. Ernst and Z. Bar-Joseph, *BMC Bioinf.*, 2006, **7**, 191.

42 J. Ernst and Z. Bar-Joseph, *BMC Bioinf.*, 2006, **7**, 191.

43 Y. Benjamini and Y. Hochberg, *J. R. Stat. Soc., B*, 1995, **57**, 289–300.

44 K. J. Wolf, J. Chen, J. Coombes, M. K. Aghi and S. Kumar, *Nat. Rev. Mater.*, 2019, **4**, 651–668.

45 D. L. Black, *Annu. Rev. Biochem.*, 2003, **72**, 291–336.

46 S. N. Thibodeau, A. J. French, S. K. McDonnell, J. Cheville, S. Middha, L. Tillmans, S. Riska, S. Baheti, M. C. Larson, Z. Fogarty, Y. Zhang, N. Larson, A. Nair, D. O'Brien, L. Wang and D. J. Schaid, *Nat. Commun.*, 2015, **6**, 8653.

47 J. A. Burdick and G. D. Prestwich, *Adv. Mater.*, 2011, **23**, H41–H56.

48 S. Khunmanee, Y. Jeong and H. Park, *J. Tissue Eng.*, 2017, **8**, 2041731417726464.